ISSN (Online) 2456-1290

International Journal of Engineering Research in Mechanical and Civil Engineering (IJERMCE)

Volume 12 Issue 12 December 2025

Numerical Investigation of Evolution of Plume Structure in Rayleigh-Benard Convection

[1] Syam Joy, [2] Franklin R John*, [3] Joshy P J, [4] Baburaj A Puthenveettil

[1][2][3] Division of Mechanical Engineering, School of Engineering, CUSAT, Cochin, India
[4] Department of Applied Mechanics & Biomedical Engineering, IIT Madras, India
Email: [1] samjoy009@gmail.com, [2] frankcusat@gmail.com, [3] pjjoshy1969@gmail.com, [4] apbraj@gmail.com

Abstract*— Numerical Investigations were carried out to study the Evolution of plume structure in Rayleigh-Benard convection at a constant Pr = 5.2 (water) and over a range of Rayleigh number $4.43 \times 10^5 < Ra_H < 7.95 \times 10^8$. Three domains of cross-section 15 cm × 15 cm and height of 5 cm, 10 cm and 20 cm were used to study the plume structure rising from the thermal boundary layer over the high-temperature bottom plate. Transient simulations were carried out in ANSYS Fluent to study the evolution of plume structures. Four different regimes where observed viz, initiation phase; characterised by stable boundary layer across the planform, impingement phase; characterised by the destabilisation of the boundary layer and impingement of bulk flow, plume formation phase; characterised by the formation of line plume from the boundary layer, and plume dynamics phase; characterised by the lateral movement of plume, formation of new plumes and merging of plumes. Total length of plume (L_p) and plume thickness (t_p) were measured from the planforms, and mean plume spacing (λ) and plume area ratio (A_p/A) were calculated using $\lambda = A/L_p$ and $A_p/A = t_p \times L_p/A$. Total length of plume was found to increase with Ra_H, whereas mean plume thickness was found to decrease with Ra_H; these opposing trends result in plume area ratio nearly independent of Ra_H.

***Index Terms*— Convection, Plume Structure, Boundary Layer, Plume Spacing, Length Of Plumes, Plume Thickness, And Plume Area Ratio**

I. INTRODUCTION

Natural convection is a type of heat transfer which occurs due to an unstable density difference created by having a high-temperature bottom plate and a low-temperature medium up top; such convections are termed Rayleigh-Bénard convections. In such convection, at high Rayleigh number (Ra_H), the thermal boundary layer over the high temperature bottom plate becomes unstable and erupts to form plume structure carrying the majority of heat from the bottom wall into the bulk Sparrow and Husar (1969), Pera and Gebhart (1973), Tamai and Asaeda (1984), Solomon and Gollub (1990). This plume structure exhibits transient behaviour, exhibiting initiation from a new point, lateral movement and merging (Gunasegarane and Puthenveettil, 2014). These plumes rise as sheets from the boundary layer (Tamai and Asaeda, 1984) and appear as line plumes in a horizontal plane adjacent to the bottom wall. The motion of high-temperature plumes rising from the boundary layer into the bulk alters the near-wall velocity and temperature profiles. A theoretical estimate of velocity and temperature profile was proposed by Ahlers *et.al* (2012), Shiskina and Thess (2009), and Theerthan and Arakeri (1998). Roten and Classen (1969) proposed a similarity solution for the temperature and velocity fields of the boundary layer in natural convection. The velocity and temperature scale for the near-wall region in natural convection is proposed by Townsend (1959), and similar scales for the bulk regime are developed by Deardorff (1970).

For a wide range of Prandtl numbers $4 < Pr < 12500$, Seki *et.al* (1978) developed correlations for the boundary layer in indirect natural convection. Plume rising from the boundary layer creates a bulk circulation which imparts shear on the boundary layer. The effect of large-scale shear on plume structures in natural convection boundary layers was studied by Puthenveettil and Arakeri (2005). The dynamics of line plumes over a range of $10^5 < Ra_H < 10$ was studied by Gunasegarane and Puthenveettil (2014), and a common lognormal distribution of merging velocity of line plumes over the range of Ra_H was found. Using order of magnitude analysis of boundary layer equations, Puthenveetil *et.al* (2011) obtained a theoretical scaling of the total length of plumes. The thickness of plumes erupting from the boundary layer was estimated to have twice the thickness of the critical velocity boundary layer (Van der Poel *et.al*, 2015), and the area ratio of plumes in a planform was also observed to be independent of Ra_H (Shevkar *et.al*, 2022). The effect of advection into the boundary layer was investigated by Nield (1969), Ramareddy *et.al* (2020), and Joshy *et.al* (2023) and observed that a weak transpiration would alter the characteristics of the boundary layer in natural convection.

Howard (1966) modelled plumes as periodic growth and eruption of the conduction layer; however, results from the experiments did not correlate with the model. Coles (1978) described the flow as a repeating pattern of steady streamwise vortices added on top of a basic flow. A numerical 2-D near-wall model of plume structure in Rayleigh-Benard convection was developed by Theerthan and Arakeri (1995); the results of this model were found to be in good agreement with the

ISSN (Online) 2456-1290

International Journal of Engineering Research in Mechanical and Civil Engineering (IJERMCE)

Volume 12 Issue 12 December 2025

experimental results. Numerical investigation of natural convection boundary layer using a three-dimensional steady laminar model was carried out by Praphul *et.al* (2019), and they observed an inverse dependence of Ra_H on mean plume spacing.

The paper is organised as follows: Three different computational domains were used to simulate the transient evolution of plumes at different Ra_H. The details of the computational domains and meshing are discussed in Section II(A). The simulation details, governing equations and boundary conditions are explained in Section II(A). The transient evolution of plumes and the dependence of plume characteristics on Ra_H and *Pr* are discussed in Section III.

II. COMPUTATIONAL MODELLING

A. Geometry Modelling and Meshing

Three different 3D models with a cross section of 15 cm × 15 cm and heights of 5 cm, 10 cm and 20 cm were used to carry out transient simulations over five orders of Rayleigh number given in Table 1. The geometry of the flow domain was modelled using SpaceClaim.

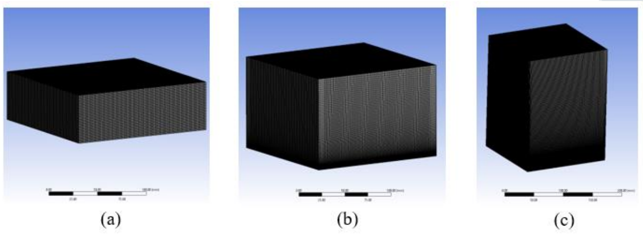

Figure 1: Three-dimensional models of the domain with a structured grid used to simulate natural convection from a high-temperature bottom wall; (a) 15 cm×15 cm×5 cm, (b) 15 cm×15 cm×10 cm and (c) 15 cm×15 cm×20 cm.

A structured grid was generated using edge sizing in ANSYS meshing. Fine mesh was generated in the near-wall region using a bias factor of 10. The concentrated fine mesh near the bottom wall can be observed in Figure 1. The grid independence was checked using a grid size of one million to 6 million cells. Grid independence was attained for a grid size of 2.5 million, with the error in Nusselt number from bottom bottom-heated wall to be less than 3%.

B. Simulation Details and Boundary Conditions

Transient simulations were carried out using ANSYS Fluent to capture the near-wall plume structures rising from the thermal boundary layer over the high-temperature bottom plate. Wall boundary conditions were assigned to the side walls and the bottom wall with a no-slip condition. The top wall was set as a pressure outlet boundary with the temperature as T_c and pressure as atmospheric pressure to simulate an open-to-atmosphere condition. The details of the isothermal boundary conditions are given in Table 1. Water is used as the working fluid across the simulations to attain a constant *Pr* of 5.2.

Table 1: Isothermal boundary conditions and domain used to simulate natural convection at different Rayleigh numbers.

Domain	Ra_H	T_h (°K)	T_c (°K)
15 cm×15 cm×5 cm	4.43×10^5	304.13	303.87
15 cm×15 cm×5 cm	3.95×10^6	305.16	302.84
15 cm×15 cm×10 cm	4.88×10^7	305.79	302.21
15 cm×15 cm×20 cm	7.95×10^8	307.65	300.35

The governing equations used to simulate natural convection from a high-temperature (T_h) bottom plate are

Continuity equation:

$$\frac{\partial u}{\partial x} + \frac{\partial v}{\partial y} + \frac{\partial w}{\partial z} = 0$$

Navier-Stokes Equation in three Dimensions

x Momentum

$$u\frac{\partial u}{\partial x} + v\frac{\partial u}{\partial y} + w\frac{\partial u}{\partial z} = -\frac{1}{\rho}\frac{\partial p}{\partial x} + \nu\left[\frac{\partial^2 u}{\partial x^2} + \frac{\partial^2 u}{\partial y^2} + \frac{\partial^2 u}{\partial z^2}\right]$$

y Momentum with the Boussinesq Approximation

$$u\frac{\partial v}{\partial x} + v\frac{\partial v}{\partial y} + w\frac{\partial v}{\partial z} = -\frac{1}{\rho}\frac{\partial p}{\partial y} + \nu\left[\frac{\partial^2 v}{\partial x^2} + \frac{\partial^2 v}{\partial y^2} + \frac{\partial^2 v}{\partial z^2}\right] + g\beta(T_h - T_c),$$

z Momentum Equation

$$u\frac{\partial w}{\partial x} + v\frac{\partial w}{\partial y} + w\frac{\partial w}{\partial z} = -\frac{1}{\rho}\frac{\partial p}{\partial z} + \nu\left[\frac{\partial^2 w}{\partial x^2} + \frac{\partial^2 w}{\partial y^2} + \frac{\partial^2 w}{\partial z^2}\right],$$

Energy Equation

$$u\frac{\partial T}{\partial x} + v\frac{\partial T}{\partial y} + w\frac{\partial T}{\partial z} = \alpha\left[\frac{\partial^2 T}{\partial x^2} + \frac{\partial^2 T}{\partial y^2} + \frac{\partial^2 T}{\partial z^2}\right].$$

SIMPLEC method was used to achieve pressure-velocity coupling, and density was modelled using the Boussinesq approximation, and the viscous model was set to laminar. A timestep size of 0.1 seconds was used to capture the transient evolution of plumes from the boundary layer, and the simulations were carried out for approximately 100 seconds.

III. RESULTS AND DISCUSSION

The evolution of plume structure is studied in a horizontal plane at a height of 2 mm from the bottom plate, along which the plume rises as a laminar sheet plume before dissipating heat into the bulk. These laminar sheet plumes appear as thick lines which move laterally and merge. The evolution of plumes is numerically recorded, converted to frames and

ISSN (Online) 2456-1290

International Journal of Engineering Research in Mechanical and Civil Engineering (IJERMCE)

Volume 12 Issue 12 December 2025

analyzed using MATLAB. The total length of the plume is measured after calibrating using a pixel-based measuring algorithm in MATLAB, plume lengths are extracted manually by tracing each plume using ginput, which records a sequence of points along the plume trajectory. The summation of the length of each segment gives the total length of the plume (L_p). The mean plume spacing (λ) is then computed using $\lambda = A/L_p$, where A is the total area of the planform. The mean thickness of the plumes (t_p) in the planform is also computed similarly by measuring segments of plumes at multiple locations where the plume thickness visibly changes, ensuring the sample accurately measures the spatial variability of plume morphology. The average plume thickness t_p is then computed by taking the average of the samples.

A. Evolution of Plumes

Four different convection regimes were observed during the evolution of plume structure from the boundary layer. The evolution begins with a stable thermal boundary layer, which appears as a high temperature region (in red) covering the entire planform at a finite height. Due to the high Ra_H, after a very short time period (t = 32 s for $Ra_H = 4.43\times10^5$), bulk flow impinges over the boundary layer due to unstable density difference, this marks the beginning of destabilization of the boundary layer as shown in (a) in Figures 2, 3, 4 and 5. The time taken for the initiation of convection increases with Ra_H. At low $Ra_H = 4.43\times10^5$, the boundary layer remains stable for about 32 seconds, whereas at a high Ra_H, convection was initiated after about 15 seconds. During this initiation phase, bulk flow impinges on multiple points over the boundary layer as shown in (b) in Figures 2, 3, 4 and 5. During this phase, the stable conductive layer at a finite height swiftly transits to sheet plumes as shown in (c) in Figures 2, 3, 4, and 5. This marks the onset of the plume dynamics phase in which plumes rise as sheets from the boundary layer, which appears as coherent lines with varying thickness, encircling the bulk flow impinging over the boundary layer. A fully developed plume field exhibits plume initiation, lateral movement and merging with adjacent plumes. Planform of plume structure at different Ra_H in plume dynamic phase at t = 100 seconds is shown in (d) in Figures 2, 3, 4 and 5.

$Ra_H = 4.43 \times 10^5$:

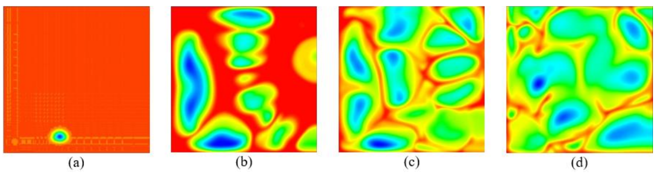

Figure 2: Evolution of plume structure with time at a constant Pr of 5.2, $Ra_H=4.43\times10^5$, and $AR=15\times15\times5$; (a)t=32s, (b) 45.4s, (c) 58.0s, and (d) 100s.

$Ra_H = 3.95 \times 10^6$:

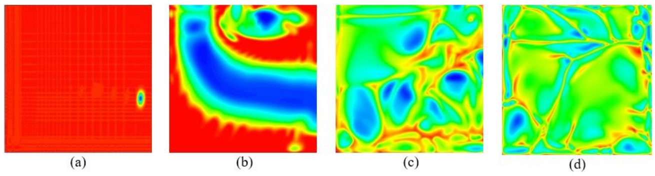

Figure 3: Evolution of plume structure with time at a constant Pr of 5.2, $Ra_H = 3.95\times10^6$, and $AR = 15\times15\times5$; (a) t = 11.9s, (b) 17.2s, (c) 34s, and (d) 100s.

$Ra_H = 4.88 \times 10^7$:

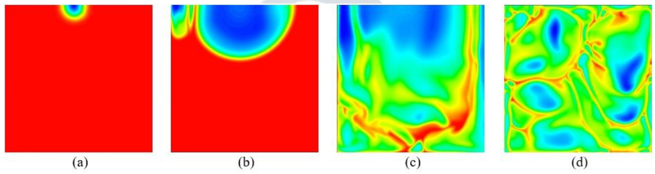

Figure 4 Evolution of plume structure with time at a constant Pr of 5.2, $Ra_H = 3.95\times10^6$, and $AR = 15\times15\times5$; (a) t = 13.9s, (b) 17.9s, (c) 37s, and (d) 100s.

$Ra_H = 7.95 \times 10^8$:

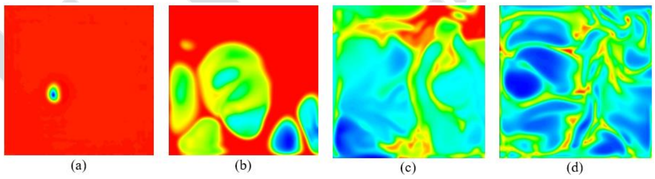

Figure 5: Evolution of plume structure with time at a constant Pr of 5.2, $Ra_H = 7.95\times10^6$, and $AR = 15\times15\times5$; (a) t = 15s, (b) 19.8s, (c) 27.5s, and (d) 100s.

B. Plume length and Mean plume spacing

Figure 6(a) shows the variation of L_p with time, and Figure 6(a) shows the variation of λ with time at different Ra_H. Even though the transient variation of Lp and λ doesn't exhibit any general trend, Lp was found to increase with Ra_H and λ was found to decrease with Ra_H. These observations are consistent with the theoretical prediction of Lp and λ by Puthenveettil *et.al* (2011).

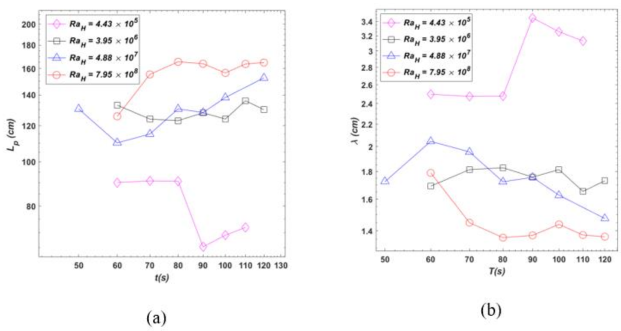

Figure 6: (a) shows the variation of plume length (L_p) with time at different Ra_H, (b) shows the variation of mean plume spacing (λ) with time at different Ra_H.

ISSN (Online) 2456-1290

International Journal of Engineering Research in Mechanical and Civil Engineering (IJERMCE)

Volume 12 Issue 12 December 2025

The increase in Lp with Ra_H is likely due to the stronger buoyancy forces at high Ra_H, accelerating the eruption of plumes from the thermal boundary layer. Strong buoyant forces also increase the shear due to circulation, which elongates the plumes before merging, thereby increasing L_p with Ra_H.

C. Plume Thickness and Plume Area Ratio

Figure 6(a) shows the transient variation of mean plume thickness (t_p) at different Ra_H. At constant Ra_H, A_p/A remains moderately constant with transient evolution of plumes, but the mean plume thickness shows a noticeable decrease with Ra_H. This observation is in line with the prediction of Van der Poel *et.al* (2015), where $t_p \sim 2\times\delta_{vc}$, where δ_{vc} is the thickness of the velocity boundary layer during onset convection. At low Ra_H, $Pr \sim 5.2$ inherently results in thicker plumes due to a thicker thermal boundary layer. The increase in Ra_H results in a reduction in δ_{vc} due to stronger near-wall shear, which in turn results in a sharper velocity gradient near the high-temperature bottom plate.

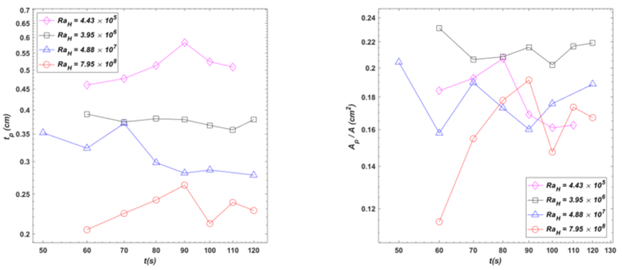

(a) (b)

Figure 7: (a) shows the variation of mean plume thickness (t_p) with time at different Ra_H, and (b) shows the variation of Plume area ratio (Ap/A) with time at different Ra_H.

Plume area ratio is calculated as $Ap/A = (t_p \times L_p)/A$; the opposing trends of t_p and L_p on Ra_H make Ap/A essentially constant with Ra_H. This can be observed from Figure 6(b), where at a constant t, Ap/A doesn't exhibit any monotonic variation with Ra_H. Similar observations were made by Prafulla *et.al* (2022), where Ap/A Rayleigh-Benard convection was observed to be a function of Pr independent of Ra_H.

IV. CONCLUSIONS

We study the evolution and characteristics of plume structure in Rayleigh-Benard convection at a constant Pr of 5.2 and over a range of Ra_H; $4.43\times10^5 < Ra_H < 7.95\times10^8$. The near-wall structures were found to be line plumes erupting from the boundary layer, which appear as coherent line plumes in a planform adjacent to the high-temperature bottom plate. The evolution of plume structure exhibits four different stages, viz, the Initiation phase, the impingement phase, the plume formation phase and the plume dynamic phase. These phases of evolution were found to have strong dependence on Ra_H, with the time required for initiation of convection and plume development decreasing significantly with an increase in Ra_H. The low Pr of water results in thicker plumes at low Ra_H, and the increase in shear due to circulation at high Ra_H results in thinner and elongated plumes. Transient measurement of L_p and t_p was carried out using pixel pixel-based measuring algorithm. L_p was found to increase with Ra_H, and t_p was found to decrease with Ra_H. This opposing trend of L_p and t_p makes the plume area ratio (Ap/A) independent of Ra_H.

REFERENCES

[1] Pera, Luciano, and Benjamin Gebhart. "Natural convection boundary layer flow over horizontal and slightly inclined surfaces." *International Journal of Heat and Mass Transfer* 16.6 (1973): 1131-1146.

[2] Tamai, Nobuyuki, and Takashi Asaeda. "Sheetlike plumes near a heated bottom plate at large Rayleigh number." *Journal of Geophysical Research: Oceans* 89.C1 (1984): 727-734.

[3] Gunasegarane, G. S., and Baburaj A. Puthenveettil. "Dynamics of line plumes on horizontal surfaces in turbulent convection." *Journal of fluid mechanics* 749 (2014): 37-78.

[4] Deardorff, James W. "Convective velocity and temperature scales for the unstable planetary boundary layer and for Rayleigh convection." *J. atmos. Sci* 27.8 (1970): 1211-1213.

[5] Theerthan, S. Ananda, and Jaywant H. Arakeri. "A model for near-wall dynamics in turbulent Rayleigh–Bénard convection." *Journal of Fluid Mechanics* 373 (1998): 221-254.

[6] Townsend, A. A. "Temperature fluctuations over a heated horizontal surface." *Journal of Fluid Mechanics* 5.2 (1959): 209-241.

[7] Husar, R. B., and E. M. Sparrow. "Patterns of free convection flow adjacent to horizontal heated surfaces." *International Journal of Heat and Mass Transfer* 11.7 (1968): 1206-1208.

[8] Ahlers, Guenter, et al. "Logarithmic temperature profiles in turbulent Rayleigh-Bénard convection." *Physical review letters* 109.11 (2012): 114501.

[9] Shishkina, Olga, and Andre Thess. "Mean temperature profiles in turbulent Rayleigh–Bénard convection of water." *Journal of fluid mechanics* 633 (2009): 449-460.

[10] Rotem, Zeev, and Lutz Claassen. "Natural convection above unconfined horizontal surfaces." *Journal of Fluid mechanics* 39.1 (1969): 173-192.

[11] Seki, Nobuhiro, Shoichiro Fukusako, and Hideo Inaba. "Visual observation of natural convective flow in a narrow vertical cavity." *Journal of Fluid Mechanics* 84.4 (1978): 695-704.

[12] Puthenveettil, Baburaj A., and Jaywant H. Arakeri. "Plume structure in high-Rayleigh-number convection." *Journal of Fluid Mechanics* 542 (2005): 217-249.

[13] van der Poel, Erwin P., et al. "Plume emission statistics in turbulent Rayleigh–Bénard convection." *Journal of fluid mechanics* 772 (2015): 5-15.

[14] Puthenveettil, Baburaj A., et al. "Length of near-wall plumes in turbulent convection." *Journal of fluid mechanics* 685 (2011): 335-364.

[15] Shevkar, Prafulla P., et al. "On separating plumes from boundary layers in turbulent convection." *Journal of Fluid Mechanics* 941 (2022): A5.

[16] Nield, D. A. "Throughflow effects in the Rayleigh-Bénard convective instability problem." *Journal of Fluid Mechanics* 185 (1987): 353-360.

[17] Ramareddy, G. V., et al. "Scaling in concentration-driven convection boundary layers with transpiration." *Journal of Fluid Mechanics* 903 (2020): A3.

[18] Joshy, P. J., Syam Joy, and Baburaj A. Puthenveettil. "Plume structures in natural convection with transpiration." *Journal of Flow Visualization and Image Processing* 30.3 (2023).

[19] Howard, Louis N. "Convection at high Rayleigh number." *Applied Mechanics: Proceedings of the Eleventh International Congress of Applied Mechanics Munich (Germany) 1964*. Berlin, Heidelberg: Springer Berlin Heidelberg, 1966.

[20] Coles, Donald. "Coherent structures in turbulent boundary layers." *Perspectives in Turbulence Studies: Dedicated to the 75th Birthday of Dr. JC Rotta International Symposium DFVLR Research Center, Göttingen, May 11–12, 1987*. Berlin, Heidelberg: Springer Berlin Heidelberg, 1987.

[21] Praphul, T., P. J. Joshy, and P. S. Tide. "Numerical Analysis of Plume Structures of Fluids on a Horizontal Heated Plate." *Journal of Heat Transfer* 141.4 (2019): 042502.